Design and Operation of Flyback CCM Inverter with Fuzzy based Discrete-Time Repetitive Control for PV Power Applications

Kanchamreddy Snehitha, R. Kiranmayi, K. Nagabhushanam

Abstract: ***In continuous conduction mode, A discrete-time repetitive controller (RC) is proposed for fly back inverter with fuzzy controller. In this paper fuzzy based repetitive controller is used due to some advantages. Such as, it reduces ripples then THD will be reduced, which has simple structure, low cost, and high efficiency. Comparing to the conventional controller the repetitive controller obtain good tracking ability and disturbance rejection and applied to flyback inverter in Continuous Conduction Mode operation. Conventional controller results in poor control performance due to the effect of the right-half-plane zero in CCM operation. To allow tracking and rejection of periodic signals within a specified frequency range the RC scheme, a low-pass filter is used. The stability of the closed loop system is derived and the zero tracking error is achieved with the stability of the closed loop system. By using the simulation results we can analyze the proposed method.***

Index Terms: Module-Integrated Converter, Right-Half-Plane Zero, Low-Pass Filter, Phase-Lead Compensation, Fuzzy Control.

I. INTRODUCTION

The feedback of the output current and the use of repetitive control algorithm are proposed in this paper for a flyback inverter that operates in CCM. The conventional controller consists of a linear controller and a feed forward controller. By using the conventional controller we get the poor control accuracy due to the Right-Half-Plane (RHP) zero which limits the available controller bandwidth.

Nowadays an AC photovoltaic (PV) system has been used mostly comparing to conventional centralized PV systems. The AC PV module system provides independent operation for each individual PV module; this design allows all modules to operate at their maximum power point (MPP) and reduces power losses caused by PV module. The AC PV module system is more reliable and easier to maintain than are centralized PV systems [1].

In the AC PV module system, to ensure maximum power extract and to provide the power to the utility grid a module-integrated converter (MIC) is attached to a single PV panel. To meet these requirements, a single-stage flyback inverter topology with an unfolding circuit has been widely used due to its number of components and its potential for high efficiency and reliability [6, 7]. Operation modes of the flyback inverter can be classified into discontinuous conduction mode (DCM) and continuous conduction mode (CCM). In fly back inverters that operate under DCM [3] the transfer function from control input to output current is a constant; thus, the output current control can be controlled easily and simply.

The flyback inverter in DCM imposes high current stress on devices; it results in decrease of conversion efficiency. In addition, the filter design becomes difficult due to the high current ripple. Compared to the DCM flyback inverters, the CCM flyback inverter has many advantages such as higher efficiency with lower current stress, easier filter design, and lower electromagnetic interference (EMI).

For eliminating the periodic disturbances in dynamic system the Repetitive Controller is widely used. In the repetitive control scheme, the present control input is obtained and this operation is performed repetitively. Hence, the repetitive controller generates the control input that ensures zero tracking error [2]. In the Repetitive Control scheme, a low-pass filter is used to disable the learning at high-frequency so that it allows tracking/rejecting periodic signals within a specified frequency range.

II. PROBLEM FORMULATION AND PRELIMINARY

Averaged model of flyback inverter in CCM operation

The circuit outline of the flyback inverter is appeared in Fig.1. The PV current is drawn from the PV panel furthermore, directed to a full wave corrected sinusoidal waveform by high frequency switching. The H-bridge is used to mitigate the output ac current into the grid.

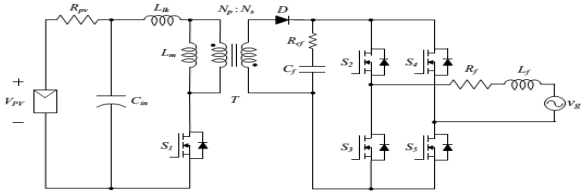

Fig.1: The circuit diagram of flyback inverter.

Photovoltaic (PV) system is used to convert sun light electrical energy to electrical energy. PV system is used mostly because it is available in free of nature. The dynamic model of PV cell is appeared in below Fig.2.

Manuscript received January 25, 2019.

Kanchamreddy Snehitha, M.Tech, Jawaharlal Nehru Technological University College of Engineering, Anantapur Andhra Pradesh, India.

Dr.R. Kiranmayi, Professor & HOD (EEE), Jawaharlal Nehru Technological University College of Engineering, Anantapur, Andhra Pradesh, India, Andhra Pradesh, India.

K. Nagabhushanam, Lecturer, Jawaharlal Nehru Technological University College of Engineering, Anantapur, Andhra Pradesh, India.

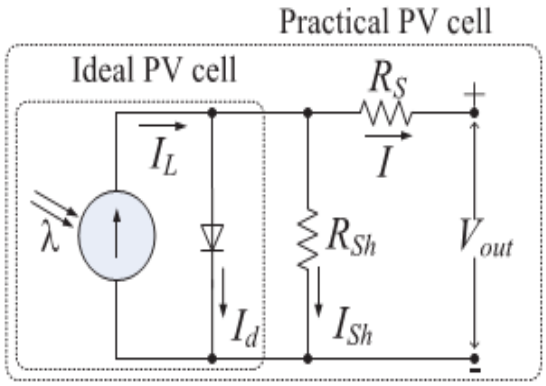

Fig.2: Equivalent electrical circuit of the PV cell.

The basic equation for the I -V characteristic of a PV cell is

$$I = I_L - I_d - I_{sh} = I_L - I_D\left[e^{\frac{QV_{oc}}{AKT}-1}\right] - \frac{V_{out}+IR_S}{R_{Sh}} \quad (1)$$

$R_s - Series\ resistance\ of\ cell\ (\Omega)$

R_{sh} – Shunt resistance of cell (Ω)

$V_{oc} - Open\ circuit\ voltage$

$I_d - Diode\ current$

I_{sh} – Shunt current(A)

I_L – Load current(A)

V_{out} – Output voltage (V)

Where I_D is the saturation current of the diode, Q is the electron charge, A is the curve fitting constant (or diode emission factor), K is the Boltzmann constant and T is the temperature on absolute scale.

The equivalent circuit of flyback inverter is shown in Fig.3.

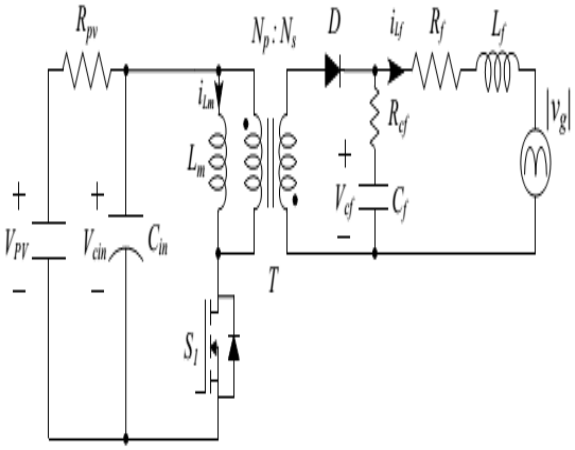

Fig.3: The Equivalent circuit of flyback inverter.

During turn-on subinterval:

$$\dot{X}(t) = \begin{bmatrix} 0 & \frac{1}{L_m} & 0 & 0 \\ -\frac{1}{C_{in}} & -\frac{1}{R_{pv}C_{in}} & 0 & 0 \\ 0 & 0 & -\frac{RC_f+R_f}{L_f} & \frac{1}{L_f} \\ 0 & 0 & -\frac{1}{C_f} & 0 \end{bmatrix} X(t) + \begin{bmatrix} 0 & 0 \\ \frac{1}{R_{pv}C_{in}} & 0 \\ 0 & -\frac{1}{L_f} \\ 0 & 0 \end{bmatrix} V(t) \quad (2)$$

$$y(t) = [0 \quad 0 \quad 1 \quad 0]X(t) \quad (3)$$

During turn-off subinterval

$$\dot{X}(t) = \begin{bmatrix} -\frac{Rc_f}{n^2L_m} & 0 & \frac{Rc_f}{nL_m} & -\frac{1}{nL_m} \\ 0 & -\frac{1}{R_{pv}C_{in}} & 0 & 0 \\ \frac{Rc_f}{nL_f} & 0 & -\frac{Rc_f+R_f}{L_f} & \frac{1}{L_f} \\ \frac{1}{nC_f} & 0 & -\frac{1}{C_f} & 0 \end{bmatrix} X(t) + \begin{bmatrix} 0 & 0 \\ \frac{1}{R_{pv}C_{in}} & 0 \\ 0 & -\frac{1}{L_f} \\ 0 & 0 \end{bmatrix} V \quad (4)$$

$$y(t) = [0\ 0\ 1\ 0]X(t) \quad (5)$$

Where i_{L_m} is the magnetizing inductor current, $v_{C_{in}}$ is capacitor voltage, i_{L_f} is the current through the output inductor, v_{C_f} is the voltage across the output capacitor. n is the transformer turns ratio of secondary to primary.

Problem formulation

In discrete-time domain the controller will be developed. To get a better connection between the flyback inverter system and the controller, the small signal model needs to be represented as the discrete-time transfer function.

By linearzing the averaged model, the small signal model can be derived as follows:

$$G_{id}(z) = \frac{\tilde{\imath}_{L_f}(s)}{\tilde{d}(s)} = \frac{a_1s^3+a_2s^2+a_3s+a_4}{s^4+b_1s^3+b_2s^2+b_3s+b_4} \quad (6)$$

Where $\tilde{\imath}_{L_f}(t)$ and $\tilde{d}(t)$ are the small ac variations of $i_{L_f}(t)$ and $D_c(t)$. By analyzing the small signal model, the system has one RHP zero, two left-half-plane (LHP) zero, and four LHP poles.

To improve the performance of the proposed method between the flyback inverter system and the controller. Utilizing in reverse contrast strategy with inspecting time of T_s, it can be depicted as:

$$G_{id}(z) = \frac{e_1z^4+e_2z^3+e_3z^2+e_4z}{z^4+f_1z^3+f_2z^2+f_3z+f_4} \quad (7)$$

Where the parameters e_j and f_j for all j = 1,…,4 are defined.

III. CONTROLLER DESIGN

Conventional Controller

The working state of the flyback inverter in CCM changes gradually during a grid period go against with a switching period; the flyback inverter can be accepted to work in quasi steady state in every moment of the matrix time frame. By expecting semi consistent state operation and utilizing volt-second adjust for the charging inductance L_m more than one exchanging period T_s, the ostensible obligation proportion $D_n(t)$ for flyback inverter in CCM can be acquired as [1]

$$D_n(t) = \frac{|v_g(t)|}{|v_g(t)|+nV_{pv}(t)} \quad (8)$$

Published By:
Blue Eyes Intelligence Engineering
& Sciences Publication

Despite the fact that $D_n(t)$ does not specifically decide the output current, the utilization of the ostensible obligation helps the flyback inverter in CCM to create the coveted yield current by easing the impact of the unsettling influences. The exchange capacity of a state feedback controller is represented as

$$C_{fb}(z) = k_p + k_i \frac{T_s}{1-z^{-1}} \qquad (9)$$

Where k_p is the proportional controller gain, k_i is the integral controller gain.

In this customary control plot, the RHP zero restrains the accessible controller data transfer capacity. Fig.4 demonstrates the Bode plot of the repaid framework when the state-feedback controller is utilized.

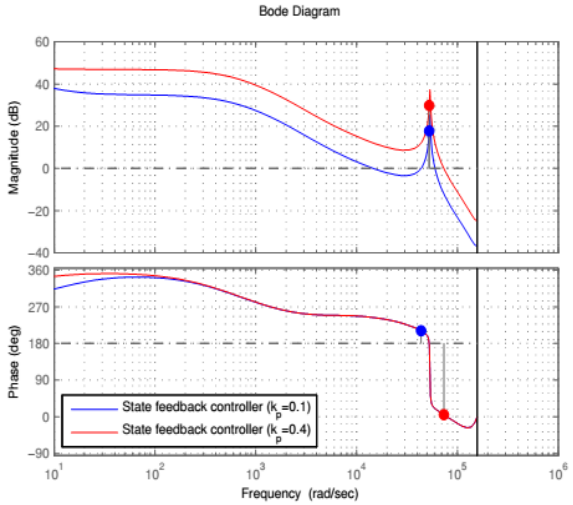

Fig.4: The Bode plot of compensated system when the state-feedback controller is used (blue); when the high-gain state-feedback controller is used (red). The dot in each magnitude Bode plot denotes the gain margin of the compensated system. The dot in each phase Bode plot denotes the phase margin of the compensated system.

As shown in Fig.4, the RHP zero makes a negative phase shift between of 20 and 1kHz. In this condition, to guarantee the following execution and aggravation dismissal, for example, the grid voltage, the high-pick up state-input controller can be utilized. It would make the flyback inverter in CCM which has the RHP zero wind up precarious. To defeat this issue, the dual controller is created in the continuation.

Repetitive controller with low-pass filter

The repetitive controller handles systems that performs the same task repetitively. In repetitive control scheme, to improve the control input for the next trial the knowledge obtained from the previous trial is used. Hence, the control input in each trial is adjusted using the tracking error signals obtained from the previous trial, and theoretically achieves zero tracking error. The concept of repetitive controller is shown in Fig.5. In the conventional control scheme, the RHP zero limits the available controller bandwidth. To achieve fast dynamical response to input signal at a specific frequency, the repetitive controller is developed.

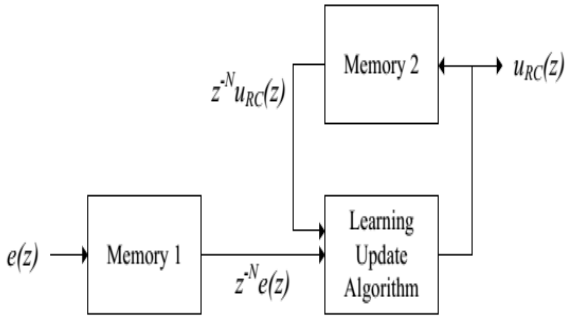

Fig.5: The concept of Repetitive Controller

In the repetitive control scheme to allow tracking/rejecting periodic signals within a specified frequency range, a low-pass filter is adopted. Moreover, to compensate for the system delay which comes from digital implementation, the phase lead compensator is used to the repetitive controller scheme.

The transfer function of the repetitive controller is

$$C_{rc}(z) = k_r \frac{z^{-N}Q(z)}{1-z^{-N}Q(z)} G_{inv}(z) \qquad (10)$$

Where k_r is the repetitive controller gain, $N = f_s/f_g$ with $f_s = \frac{1}{T_s}$ being the sampling frequency and f_g being the frequency of reference, Q(z) is the low-pass filter, and $G_{inv}(z)$ is the inverse function of the system. For tracking/rejecting periodic signals within a specified frequency range and easy implementation, Q(z) is chosen as moving average filter with zero phase shift:

$$Q(z) = \sum_{i=0}^{p} \alpha_i z^i + \sum_{i=1}^{p} \alpha_i z^{-i} \qquad (11)$$

Where $\alpha_0 + 2\sum_{i=1}^{p} \alpha_i$ is the number of samples to be used for filtering. Here, a first order filter $Q(z) = \alpha_1 z + \alpha_0 + \alpha_1 z^{-1}$ is used; as 0 becomes larger, the cutoff frequency of Q(z) becomes higher. Due to the system uncertainty, the system delay, and the unknown disturbance, $G_{inv}(z)$ cannot be precisely implemented. Here, to compensate even the effect of the system delay, G_{inv} are set as

$$G_{inv}(z) = z^m \qquad (12)$$

where m is the prediction index. With the complete repetitive controller, the overall control system is shown in Fig.6.

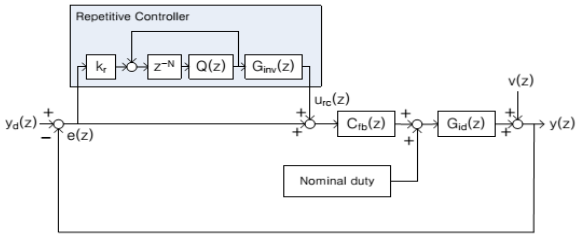

Fig.6: The schematic diagram of overall control system. $y_d(z)$is the reference, e(z) is the error,

$u_{rc}(z)$ is the repetitive control input, $v(z) = [V_{pv}(z), |v_g|]^T$

Fig.7 demonstrates the Bode plot of the compensated system when the repetitive controller is utilized. Utilized parameters are recorded in Table I.

To maintain a strategic distance from the control at a high-recurrence and stifle crucial and low-arrange music parts, the low-pass channel is received in the monotonous control conspire. It cripples the learning at high-recurrence.

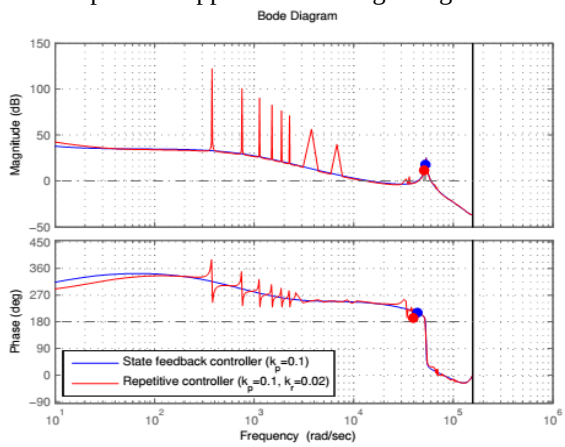

Fig.7: The Bode plot of compensated system when the state-feedback controller is used (blue); when the repetitive controller with low-pass filter is used (red). The dot in each magnitude Bode plot denotes the gain margin of the compensated system. The dot in each phase Bode plot denotes the phase margin of the compensated system.

Stability Analysis

In the repetitive control system shown in Fig.5, the input output relationship of the flyback inverter in CCM is described as

$$y(z) = G(z)y_d(z) + S(z)v(z) \qquad (13)$$

where $G(z)y_d(z)$ is the command input response and $S(z)v(z)$ is the disturbance response; G(z) is the transfer function from reference to output and S(z) is the sensitivity function; G(z) and S(z) are represented as

$$G(z) = \frac{y(z)}{yd(z)} = \frac{[1-Q(z)z^{-N}(1-k_r z^m)]G_C(Z)}{[[1-Q(z)z^{-N}(1-k_r z^m)]G_C(Z)]} \qquad (14)$$

$$S(z) = \frac{y(z)}{u(z)} = \frac{[1-Q(z)z^{-N}](1-G_C(Z))}{1-Q(z)z^{-N}(1-k_r z^m G_C(Z))} \qquad (15)$$

where

$G_c(z) = C_{fb}(z)G_{id}(z)/\big(1 + C_{fb}(z)G_{id}(z)\big)$. The relationship between the error $e(z) = y(z) - y_d(z)$and the reference $y_d(z)$ and disturbance v(z) can be obtained as

$$\frac{e(z)}{w(z)} = \frac{(1-Q(z)z^{-N})(1-G_C(Z))}{1-Q(z)z^{-N}(1-k_r z^m G_c(z))}$$

The transfer function e(z)/w(z) can be written as three systems connected in cascade. The term $1 - Q(z)z^{-N}$is a low-pass filter and a time delay, and so it is stable.

IV. FUZZY LOGIC CONTROLLER

In FLC, essential control activity is dictated by an arrangement of phonetic standards. These standards are controlled by the framework. Since the numerical factors are changed over into semantic factors, scientific displaying of the framework isn't required in FC.

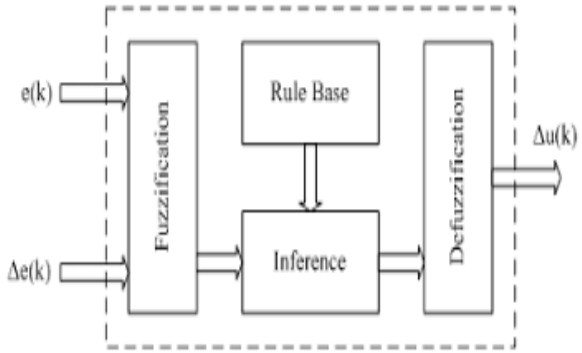

Fig.8: Fuzzy logic controller

The FLC involves three sections: fuzzification, obstruction motor and defuzzification. The FLC is described as

1. Seven fuzzy sets for each info.
2. Triangular enrollment capacities for effortlessness.
3. Fuzzification utilizing consistent universe of talk. iv. Suggestion utilizing Mamdani's 'min' administrator
4. Defuzzification utilizing the tallness strategy.

TABLE I: Fuzzy Rules

e/Δe	NB	NM	NS	ZE	PS	PM	PB
NB	NB	NB	NB	NM	NS	ZE	PS
NM	NB	NB	NB	NM	NS	PS	PM
NS	NB	NB	NM	NS	ZE	PS	PM
ZE	NB	NM	NS	ZE	PS	PM	PB
PS	NM	NS	ZE	PS	PM	PB	PB
PM	NS	ZE	PS	PM	PB	PB	PB
PB	ZE	PS	PM	PB	PB	PB	PB

Fuzzification: Enrollment work esteems are doled out to the etymological factors, utilizing seven fuzzy subsets: NB (Negative Big), NM (Negative Medium), NS (Negative Small), ZE (Zero), PS (Positive Small), PM (Positive Medium), and PB (Positive Big). The Partition of fuzzy subsets and the state of enrollment CE(k) E(k) work adjust the take care of business to fitting framework. The estimation of information mistake and change in blunder are standardized by an info scaling factor. In this framework the information scaling factor has been outlined with the end goal that information esteems are between - 1 and +1. The triangular state of the participation capacity of this plan presumes that for a specific E(k) contribution there is just a single predominant fuzzy subset. The information blunder for the FLC is given as

$$E(k) = \frac{P_{ph(k)} - P_{ph(k-1)}}{V_{ph(k)} - V_{ph(k-1)}} \qquad (16)$$

$$CE(k) = E(k) - E(k\text{-}1) \qquad (17)$$

Inference Method: A few arrangement strategies, for example, Max– Min and Max-Dot have been proposed in the writing. In this paper Min technique is utilized. The yield enrollment capacity of each control is given by the base administrator and greatest administrator. Table 1 demonstrates control base of the FLC.

Defuzzification: As a plant more often than not requires a non-fuzzy estimation of control, a defuzzification arrange is required.

Published By:
Blue Eyes Intelligence Engineering
& Sciences Publication

To register the yield of the FLC, „height" strategy is utilized and the FLC yield alters the control yield. Further, the yield of FLC controls the switch in the inverter. In UPQC, the dynamic power, reactive power, terminal voltage of the line and capacitor voltage are required to be kept up. Keeping in mind the end goal to control these parameters, they are detected and contrasted and the reference esteems. To accomplish this, the enrollment elements of FC are: mistake, change in blunder and yield

The set of FC rules are derived from

$$u=-[\alpha E + (1-\alpha)*C] \quad (18)$$

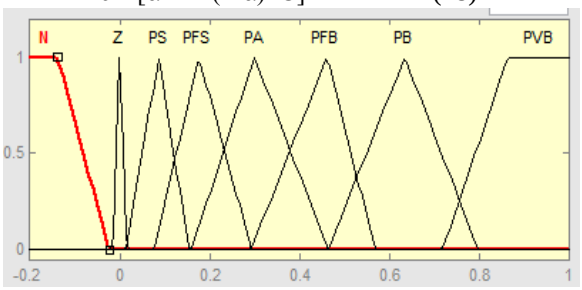

Fig.9: Input error as membership functions

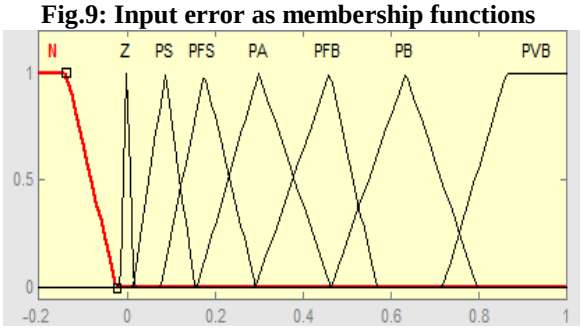

Fig.10: Change as error membership functions

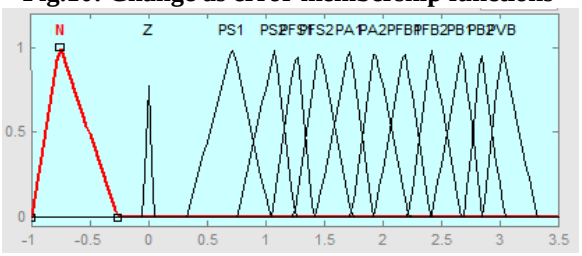

Fig.11: Output variable Membership functions

Where α is self-adjustable factor which can regulate the whole operation. E is the error of the system, C is the change in error and u is the control variable.

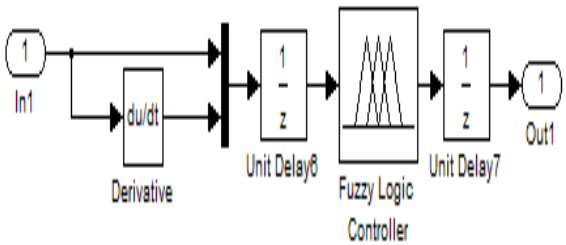

Fig.12: Fuzzy logic controller in simulation

V. SIMULATION RESULTS

To exhibit the performance of the proposed controller, simulation. The flyback inverter in CCM mode parameters are input voltage V_{pv} = 60 V, framework voltage V_g = 220 V_{rms}, and evaluated yield control P_o = 200 W. The real parameters for proposed inverter are recorded in Table I. The aggregate framework design is appeared in Fig.13.

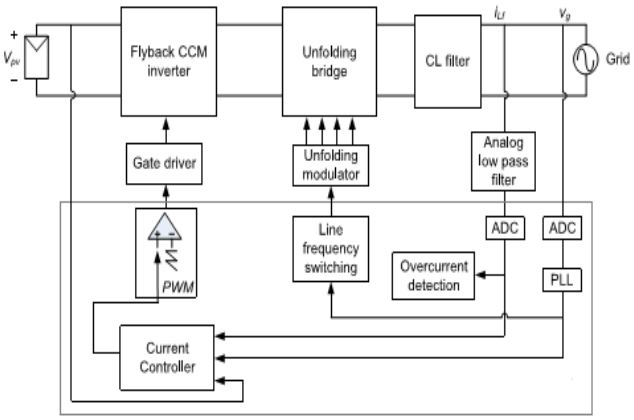

Fig.13: Configuration of the proposed control system. PWM stands for pulse width modulation. ADC stands for analog-to-digital converter.

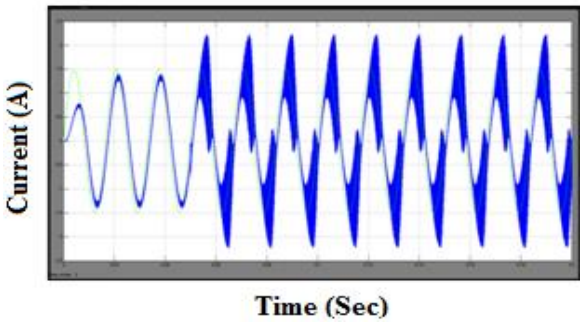

(a)

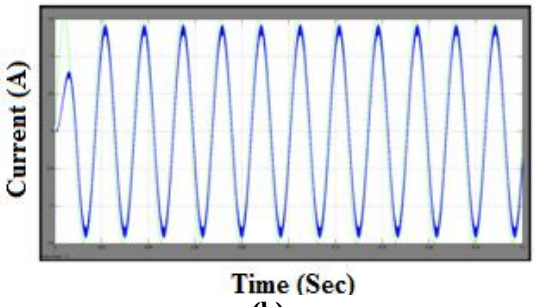

(b)

Fig.14: The waveforms of desired output current (a) When the conventional controller is used. (b) When the proposed controller is used.

Fig.14(a) Demonstrates waveforms of the reference and yield current when regular control plot with straight controller in addition to feed forward controller is connected.

Fig.14(b) Indicates waveforms of the current with better performance when proposed control conspire is connected.

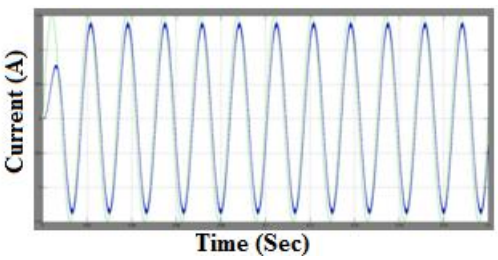

Fig.15: The waveforms of desired output current when fuzzy controller is used.

Published By:
Blue Eyes Intelligence Engineering
& Sciences Publication

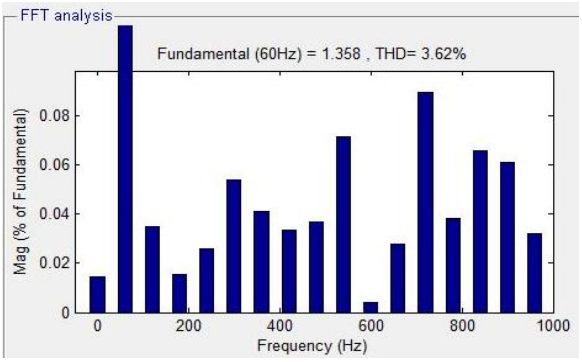

Fig.16: Total harmonic distortion with Repetitive Controller

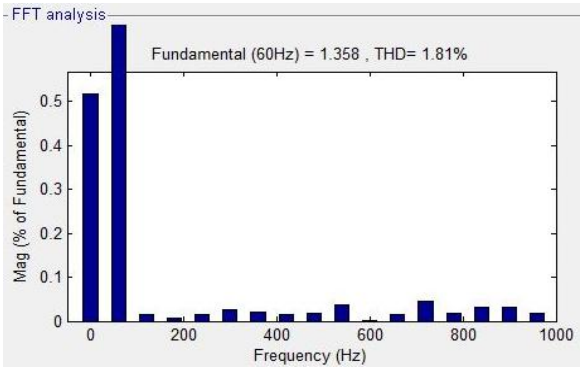

Fig.17: Total harmonic distortion with fuzzy controller

VI. CONCLUSION

In this paper, the feedback of the output current and the use of repetitive control algorithm are proposed wit fuzzy controller for a flyback inverter that operates in CCM. which has simple design, minimal effort, and high effectiveness. Comparing with the conventional controller the proposed controller eliminates the ripples, then total harmonic distortion also reduced. To achieve the accurate tracking performance and disturbance rejection, the repetitive controller is developed and applied to flyback inverter in CCM operation. The low pass filter is used to rejecting periodic signals within a specified frequency range. The stability of closed-loop system is derived and the zero tracking error is achieved. The simulation results verify the proposed control method by using the simulation results.

REFERENCES

1. F. F. Edwin, W. Xiao, and V. Khankikar, "Dynamic displaying and control of interleaved flyback module-incorporated converter for PV control applications," IEEE Trans. Ind. Electron., vol. 61, no. 3, pp. 1377-1388, Mar. 2014.
2. S. B. Kjaer, J. K. Pedersen, and F. Blaabjerg, "An audit of single-stage framework associated inverters for photovoltaic modules," IEEE Trans. Ind. Appl., vol. 41, no. 5, pp. 1292-1306, Sep./Oct. 2005.
3. Y. H. Kim, J. W. Jang, S. C. Shin, and C. Y. Won, "Weighted-proficiency upgrade control for photovoltaic AC module interleaved flyback inverter utilizing a synchronous rectifier," IEEE Trans. Power Electron., vol. 29, no. 12, pp. 6481-6493, Dec. 2014.
4. G. Petrone, G. Spagnuolo, and M. Vitelli, "A simple system for conveyed MPPT PV applications," IEEE Trans. Ind. Electron., vol. 59, no. 12, pp. 4713-4722, Dec. 2012
5. Y. Li and R. Oruganti, "A flyback-CCM inverter conspire for photovoltaic AC module application," in Proc. Australasian Univ. Power Eng. Conf. (AUPEC), 2008, pp 1-6.
6. N. Kasa, T. Iida, and L. Chen, "Flyback inverter controlled by sensorless current MPPT for photovoltaic power framework," IEEE Trans. Ind. Electron., vol. 52, no. 4, pp. 1145-1152, Aug. 2005.
7. N. Sukesh, M. Pahlevaninezhad, and P. K. Jain, "Examination and execution of a solitary stage flyback PV microinverter with delicate exchanging," IEEE Trans. Ind. Electron., vol. 61, no. 4, pp. 1819-1833, Apr. 2014.
8. Z. Zhang, X. F. He, and Y. F. Liu, "An ideal control strategy for photovoltaic lattice tide-interleaved flyback microinverters to accomplish high productivity in wide load extend," IEEE Trans. Power Electron., vol. 28, no. 11, pp. 5074-5087, Nov. 2013.
9. H. Hu, S. Harb, N. H. Kutkut, Z. J. Shen, and I. Batarseh, "A singlestage microinverter without utilizing electrolytic capacitors," IEEE Trans. Power Electron., vol. 28, no. 6, pp. 2677-2687, Jun. 2013.
10. R. W. Erickson and D. Maksimovic, "Essentials of Power gadgets," Springer Science and Business Media, 2007.